Journal of Alloys and Compounds 507 (2010) L17–L20

Contents lists available at ScienceDirect

Journal of Alloys and Compounds

journal homepage: www.elsevier.com/locate/jallcom

Letter

Thermodynamic properties of RhO_2

K.T. Jacob*, Debadutta Prusty

Department of Materials Engineering, Indian Institute of Science, C.V. Raman Avenue, Bangalore 560012, India

ARTICLE INFO

Article history:
Received 21 June 2010
Received in revised form 14 July 2010
Accepted 16 July 2010
Available online 5 August 2010

Keywords:
Thermodynamic properties
Enthalpy
Entropy
Electromotive force (emf)
Decomposition temperature
Stability

ABSTRACT

A solid-state electrochemical cell, with yttria-stabilized zirconia as the electrolyte and pure O_2 gas at 0.1 MPa as the reference electrode, has been used to measure the oxygen chemical potential corresponding to the equilibrium between β-Rh_2O_3 and RhO_2 in the temperature range from 850 to 1050 K. Using standard Gibbs energy of formation of β-Rh_2O_3 available in the literature and the measured oxygen potential, the standard Gibbs free energy of formation of RhO_2 is derived as a function of temperature:

$$\Delta G_f^\circ(RhO_2)(\pm 71)/\text{J mol}^{-1} = -238,418 + 179.89T$$

Using an estimated value of ΔC_p° for the formation reaction of RhO_2 from its elements, the standard enthalpy of formation, standard entropy and isobaric heat capacity of RhO_2 at 298.15 K are evaluated: ΔH_f° (298.15 K)(±164)/kJ mol^{-1} = −244.94, S° (298.15 K)(±3.00)/J mol^{-1} K^{-1} = 45.11 and C_p° (298.15 K)(±2.6)J mol^{-1} K^{-1} = 64.28.

1. Introduction

Rhodium metal supported on alumina is a selective catalyst for steam reforming of aromatic compounds [1]. The metal is also used in automotive three-way catalysts for the oxidation of CO and hydrocarbons and reduction of NO_x present in exhaust gases [2,3]. The major role of the catalyst in the oxidation of CO is to dissociate O_2 molecules, which occurs spontaneously in the adsorption process. The "free" oxygen atoms on the surface react with adsorbed CO to form CO_2 [4]. Gustafson et al. [4] have shown that a thin RhO_2 surface oxide film forms on metal Rh prior to the bulk Rh_2O_3 with corundum structure. Increase in CO_2 production has been correlated with the presence of the thin RhO_2 surface films. Bulk Rh_2O_3 appears to poison the oxidation of CO. Thus, the ability to predict the effect of temperature and oxygen pressure on the stability of rhodium and its oxides is important for industrial catalytic processes. Further, anodic film formed on Rh electrode in an alkaline solution exhibits reversible color change between lemon yellow ($Rh_2O_3{\cdot}5H_2O$) and olive green ($RhO_2{\cdot}2H_2O$) by successively reversing applied potentials [5]: an effect attributed to change in the oxidation state of metal ions.

The stable oxide phase in equilibrium with metallic Rh is Rh_2O_3 [6], which exists in two polymorphic forms: α-Rh_2O_3 or the low-temperature form having corundum structure (space group *R*3*c*) with lattice parameters *a* = 0.5127 nm and *c* = 1.3853 nm [JCPDS file no. 00-043-1025], and β-Rh_2O_3 or the high-temperature form exhibiting orthorhombic structure (space group *Pbca*) with *a* = 0.51472 nm, *b* = 0.54379 nm and *c* = 1.4691 nm [JCPDS file no. 00-043-0009]. The oxidation of Rh always results in the formation of high-temperature form of Rh_2O_3. Thermodynamic properties of β-Rh_2O_3 are now well established [6,7]. Lower oxides, Rh_2O and RhO, identified by Wöhler and Jochum [8] in the early study of the system Rh–O, have not been confirmed by subsequent investigators. RhO_2, which is stable at high oxygen pressures, has the rutile structure (space group $P4_2/mnm$) with (*a* = 0.44862 nm and *c* = 0.30884 nm) [JCPDS file no. 01-074-2385]. Muller and Roy [9] have studied the stability of the Rh oxides as a function of temperature in the range from 723 to 1273 K and oxygen pressure in the range $0.21 \le P_{O_2}/P^o \le 4000$, where P^o is the standard atmospheric pressure. The results are neither sufficiently reproducible nor accurate to derive thermodynamic data. Although rhodium is generally present in the trivalent state oxides especially at elevated temperatures, there are indications of the presence of tetravalent rhodium in some complex oxides, especially spinel solid solutions.

Norman et al. [10] have detected both RhO and RhO_2 species in the gas phase using Knudsen cell mass-spectrometry, with constant flow of oxygen into the Knudsen cell at partial pressures varying from $10^{-5} < P_{O_2}/P^o < 10^{-3}$. These experiments were conducted in the temperature range from 1903 to 2173 K. Alcock and Hooper [11] studied the volatility of Rh as a function of oxygen partial pressure from 1273 to 1773 K. They show that RhO_2 is the predominant gas species.

Experimentally determined thermodynamic properties of RhO_2 have not been reported in the literature. Heat capacity of RhO_2 at 298.15 K has been estimated by Hurst and Harrison [12] using mod-

* Corresponding author. Tel.: +91 80 2293 2494; fax: +91 80 2360 0472.
E-mail addresses: katob@materials.iisc.ernet.in, ktjacob@hotmail.com (K.T. Jacob).

0925-8388/$ – see front matter © 2010 Elsevier B.V. All rights reserved.
doi:10.1016/j.jallcom.2010.07.179

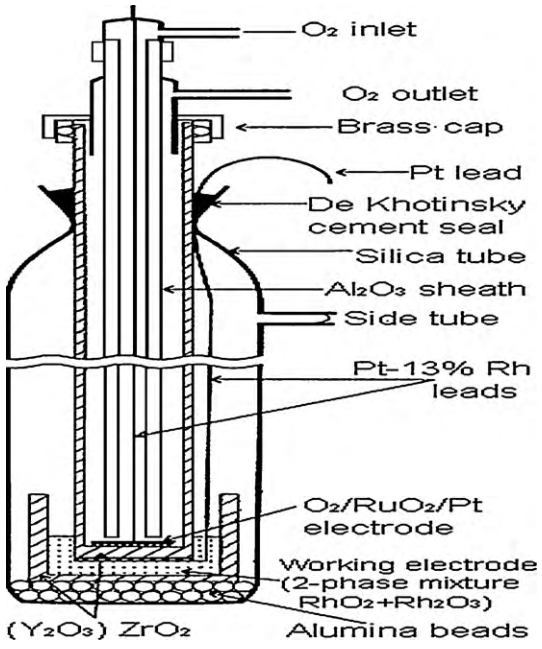

Fig. 1. Schematic diagram of the cell assembly used for electrochemical measurement.

ified Kopp's rule as 53.47 J mol^{-1} K^{-1} and by Leitner et al. [13] as 55 J mol^{-1} K^{-1}. Because of the absence of data on RhO_2 in all thermodynamic data compilations, an experimental determination of the standard Gibbs free energy of RhO_2 as a function of temperature was undertaken. The oxygen chemical potential associated with the equilibrium between β-Rh_2O_3 and RhO_2 was measured using a solid-state cell. The standard enthalpy of formation and standard entropy of RhO_2 at 298.15 K were evaluated.

2. Experimental methods

2.1. Sample preparation

Dark grey β-Rh_2O_3 was prepared by oxidation of fine powder of metallic Rh at 1323 K in pure oxygen gas at ambient pressure. RhO_2 was prepared by thermal decomposition of $Rh_2O_3{\cdot}5H_2O$ at 923 K. The product was heated at 1073 K for ~50 ks in pure oxygen gas at a pressure $P_{O_2}/P^o = 10$, where P^o is the standard atmospheric pressure. Formation of both oxides was confirmed by XRD. The composition of both compounds was verified by reductive gravimetry (mass loss during reduction by hydrogen gas) at 1073 K.

2.2. Electrochemical measurements

The reversible emf of the solid-state electrochemical cell: Pt – 13 % Rh, β - Rh_2O_3 + RhO_2/(Y_2O_3)ZrO_2/O_2(0.1 MPa), (RuO_2), Pt – 13 % Rh, was measured as a function of temperature in the range 850–1050 K. The cell is written such that the right hand electrode is positive. Yttria-stabilized zirconia tube functioned as the solid electrolyte with predominant oxygen ion conduction ($t_{ion} > 0.999$) under the experimental conditions encountered in this study.

The cell assembly used for electrochemical measurements is shown in Fig. 1. The yttria-stabilized zirconia tube used as the solid electrolyte was leak tested and found to be impervious. A coating of RuO_2 was applied on flat inner surfaces of the closed-end tube so that it would serve as a low interfacial impedance electrode at reduced operating temperatures [14]. Drops of 10% aqueous solution of $RuCl_3$ was dropped inside the tube. After drying, the tube was heated in air at 1073 K for 300 s. A highly adherent black porous film of RuO_2 is obtained by this treatment. The half-spherical type RuO_2 particles attached to the solid electrolyte catalyzed the conversion of diatomic oxygen molecules from gas phase to oxygen ions in the solid electrolyte. A platinum mesh is placed over the RuO_2 electrode. A Pt–13%Rh wire, spot welded to the mesh, was used as an electrical lead. Good contact with the electrolyte tube was ensured by pressing the platinum mesh against the RuO_2 electrode with an alumina tube. Oxygen gas at 0.1 MPa pressure was flown over the RuO_2 electrode at a flow rate of 1.5 ml s^{-1}.

A mixture of β-Rh_2O_3 and RhO_2 in the molar ratio 1:1.5 was placed in a yttria-stabilized zirconia crucible, with a Pt–13%Rh wire embedded in the mixture. The solid electrolyte tube was pressed against the two-phase mixture as shown in the figure. The oxygen chemical potential associated with the phase mixture of β-Rh_2O_3 and RhO_2 was measured by the solid-state cell. The assembly was enclosed in an outer quartz tube. At the cold end, the gap between the neck of the quartz tube and the zirconia tube was closed with De Khotinsky cement as shown in the diagram. After assembling the cell, the quartz tube is evacuated through a side arm to a pressure of 0.1 Pa and then flame sealed. During the experiment, the equilibrium oxygen partial pressure is established inside the quartz tube by the dissociation of RhO_2 into β-Rh_2O_3. The oxygen partial pressure for the dissociation of β-Rh_2O_3 to Rh and O_2 is considerably lower.

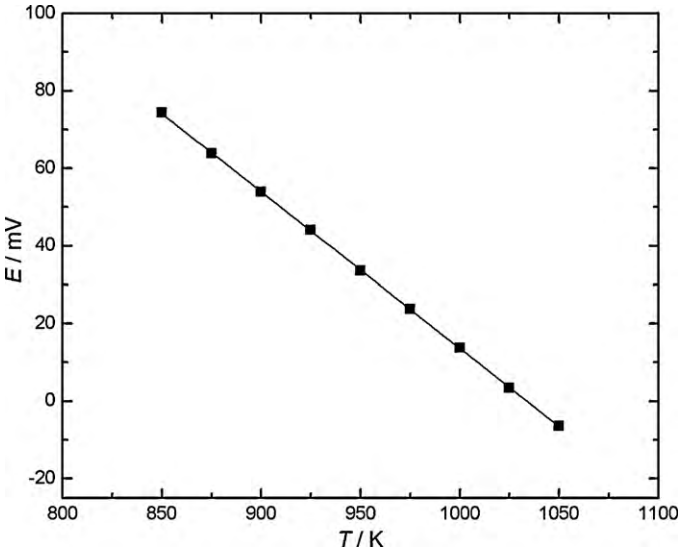

Fig. 2. Variation of the emf of the solid-state electrochemical cell with temperature.

The reversibility of the emf was established by microcoulometric titration in either direction. A small quantity of current (~25 μA for 200 s) was passed through the cell using an external potential source and then the open-circuit emf was recorded as a function of time. In each case, the emf was found to gradually return to the steady state value before the titration. Since the emf returned to the same value after successive essentially infinitesimal displacements from equilibrium in both directions, the reversibility was confirmed. The emf was also found to be insensitive to changes in the flow of oxygen gas through the solid electrolyte tube by a factor 2× and reproducible on cycling the temperature of the cell. After the emf measurements, the cell was cooled and the cell components were examined. There was no evidence of reaction between RuO_2 and Pt at the reference electrode. The working electrode was examined by optical and scanning electron microscope and XRD before and after the experiment. There was no change in the characteristic patterns of the two oxides during the experiment; observed was only a change in the relative concentration of the two phases caused by partial decomposition of RhO_2 to Rh_2O_3 during experiment to establish the equilibrium oxygen partial pressure inside the evacuated quartz tube.

3. Results and discussion

The reversible emf of the solid-state cell is plotted as a function of temperature in Fig. 2. The emf decreases linearly with increasing temperature. The least squares regression analysis gives:

$$E(\pm 0.39)/\text{mv} = 417.01 - 0.4034T \quad (1)$$

where the uncertainty limit corresponds to twice the standard deviation (2σ). The corresponding uncertainty in the temperature-independent term is ±1.9 and in the temperature-dependent term is ±0.002. The open-circuit potential of the concentration cell is expressed as

$$E = \frac{RT}{4F} \ln\left(\frac{P^o_{O_2}}{P_{O_2}}\right) \quad (2)$$

where P_{O_2} and $P^o_{O_2}$ are the oxygen pressures at the working electrode and the reference electrode, respectively, F is the Faraday constant, and R the gas constant. As pure oxygen at 0.1 MPa was used as the reference electrode, the emf directly gives the oxygen potential ($\Delta\mu_{O_2} = RT \ln P_{O_2}$) at the working electrode, which

is defined by the reaction:

$$0.5\beta\text{-}Rh_2O_3 + 0.25O_2 \rightarrow RhO_2 \quad (3)$$

The standard Gibbs energy of formation of RhO_2 from oxygen and β-Rh_2O_3 according to reaction (3) is related to oxygen potential:

$$\Delta G_3^\circ(\pm 37)/\text{J mol}^{-1} = 0.25\Delta\mu_{O_2} = 0.25RT \ln P_{O_2} = -FE$$
$$= -40,235 + 38.89T \quad (4)$$

The standard Gibbs free energy of formation of β-Rh_2O_3 obtained from recent measurement [6] in the temperature range from 873 to 1300 K is:

$$\Delta G_f^\circ(\beta\text{-}Rh_2O_3)(\pm 120)/\text{J mol}^{-1} = -396,365 + 282.0T \quad (5)$$

Combining Eqs. (4) and (5), the standard Gibbs energy of formation of RhO_2 can be computed as

$$Rh(s) + O_2 \rightarrow RhO_2 \quad (6)$$

$$\Delta G_f^\circ(RhO_2)(\pm 71)/\text{J mol}^{-1} = \Delta G_3^\circ + 0.5\Delta G_f^\circ(\beta - Rh_2O_3)$$
$$= -238,418 + 179.89T \quad (7)$$

The temperature-independent term in the above equation gives the standard enthalpy of formation ($\Delta H_f^\circ(\pm 0.16)/\text{kJ mol}^{-1} = -238.42$) of RhO_2 according to reaction (6) at the mean experimental temperature of 950 K. The temperature-dependent term with change in sign gives the corresponding entropy of formation ($\Delta S_f^\circ(\pm 0.15)/\text{J mol}^{-1}\,\text{K}^{-1} = -179.89$) at the same temperature. To calculate ΔH_f° (298.15 K) and ΔS_f° (298.15 K), the following relations are used:

$$\Delta H_f^\circ(T) = \Delta H_f^\circ(298.15\,\text{K}) + \int_{298.15}^{T} \Delta C_p^\circ dT \quad (8)$$

$$\Delta S_f^\circ(T) = \Delta S_f^\circ(298.15\,\text{K}) + \int_{298.15}^{T} \frac{\Delta C_p^\circ}{T} dT \quad (9)$$

An estimated value of $\Delta C_p^\circ(\pm 2.5)/\text{J mol}^{-1}\,K^{-1} = 10$ is used for the evaluation of enthalpy and entropy of formation at 298.15 K. The estimated value is slightly larger than that for the isostructural compound TiO_2 at 900 K (8.25 J $\text{mol}^{-1}\,\text{K}^{-1}$) [15], but smaller than an average value of 12.55 J $\text{mol}^{-1}\,\text{K}^{-1}$ recommended by Kubaschewski and Alcock [16] for reactions similar to (6). The corresponding value of ΔC_p° of RhO_2 at 298.15 K is 64.28 (±2.6) J $\text{mol}^{-1}\,\text{K}^{-1}$, which is considerably larger than the estimated values given in the literature [7,8]. The derived thermodynamic properties at 298.15 K are: ΔH_f° (298.15 K)(±1.64) kJ $\text{mol}^{-1} = -244.94$, and ΔS° (298.15 K)(±2.9)/J $\text{mol}^{-1}\,\text{K}^{-1} = -191.48$.

The standard entropy of RhO_2 is obtained as ΔS° (298.15 K)(±2.9)/J $\text{mol}^{-1}\,\text{K}^{-1} = -191.48$ by using values for standard entropies of Rh and O_2 at 298.15 K from Pankratz [15]. It would be useful to confirm the derived values by calorimetric measurements of enthalpy of formation and heat capacity as a function of temperature.

Temperatures for the decomposition of RhO_2 according to reaction (3) can be computed from the data measured in this study as a function of temperature. The decomposition temperature in pure diatomic oxygen gas at ambient pressure is 1035 (±1) K; decomposition to β-Rh_2O_3 occurs at 955 (±1) K in dry air. Decomposition temperatures at any oxygen partial pressure can be computed from Eq. (4).

The standard Gibbs free energies of formation of the two stable solid oxides (Rh_2O_3 and RhO_2) and two vapor species (RhO and RhO_2) identified in the system Rh-O are plotted as a function of temperature in Fig. 3 à la Ellingham, Richardson and Jeffes. Data for solid Rh_2O_3 is from reference [6], for solid RhO_2 from this study, for RhO gas from reference [17] and for RhO_2 from reference [11]. It is seen that the gas species RhO is very unstable and can be detected by mass-spectrometry only at very high temperatures [10]. Species RhO_2 is relatively more stable. At the highest temperature used in this study (1050 K), the vapor pressure of RhO_2 species over pure solid RhO_2, $P_{RhO_2}/P^o = 1.74 \times 10^{-11}$, which is negligible. Thus, experimental measurement of the decomposition oxygen potential of solid RhO_2 to Rh_2O_3 is not affected by volatile species containing rhodium present in the system. Data for RuO_2 [18] displayed in Fig. 3 shows that the oxide is more stable than Rh_2O_3 and will not be reduced by platinum with which it is in contact at the reference electrode.

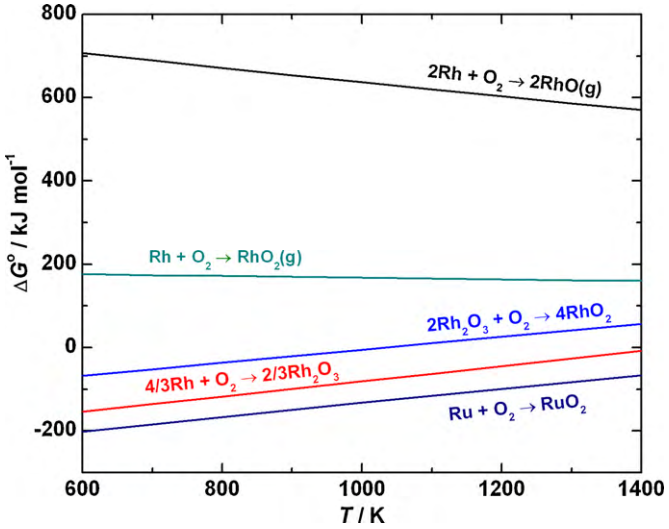

Fig. 3. Variation of the standard Gibbs energy of formation of oxides of Rh and Ru as a function of temperature.

It is informative to compare the relative stability of the two solid oxides, β-Rh_2O_3 and RhO_2. The enthalpy of formation of β-Rh_2O_3 per oxygen atom at 298.15 K (−135.18 kJ mol^{-1}) [11] is more negative than for RhO_2 (−122.47 kJ mol^{-1}). The metal to oxygen bond strength in transition metal oxides can be attributed to the hybridization between M-4d and O-2p states. The optimal filling or the bonding states in the metal–oxygen hybridization complex controls the relative stability of rhodium oxide in the two different stoichiometries. In rutile-type RhO_2, part of the d-electrons associated with Rh^{4+} fill anti-bonding states (Rh–d_{eg}–O_{px+pz} bands) leading to weaker Rh–O bonds. As discussed by Grillo [19], the relative stability of Rh_2O_3 can be attributed to the energy gap between occupied bonding (Rh–dt_{2g}–O_p) and empty anti-bonding (Rh–d_{eg}–O_{py}) states, resulting in an insulating phase with electron valence charge density dominated by the t_{2g} symmetry. Thus, the lower Rh–O bond energy in RhO_2 compared to Rh_2O_3 arises from the differences in Rh–O hybridization efficiency in the two structures.

4. Summary and conclusions

Thermodynamic properties of RhO_2 were determined using a solid-state cell at high temperatures. For the RhO_2 formation reaction:

$$Rh(s) + O_2 \rightarrow RhO_2$$

the standard Gibbs free energy change in the temperature range from 850 to 1050 K can be represented by the equation:

$$\Delta G_f^\circ(RhO_2)(\pm 71)/\text{J mol}^{-1} = -238,418 + 179.89T$$

Using an estimated value for ΔC_p°, the standard enthalpy of formation and standard entropy of RhO_2 from elements at 298.15 K were evaluated: ΔH_f° (298.15 K)($\pm$1.64)/kJ mol^{-1} = – 244.94 and S° (298.15 K)($\pm$3.00)/J mol^{-1} K^{-1} = 45.11.

Acknowledgements

K.T. Jacob wishes to thank the Indian National Academy of Engineering, New Delhi, for support as INAE Distinguished Professor. Debadutta Prusty is grateful to the Indian Academy of Sciences, Bangalore, for the award of summer research fellowship at Indian Institute of Science.

References

[1] D. Duprez, Appl. Catal. A: Gen. 82 (1992) 111–157.
[2] K.C. Taylor, Catal. Rev. Sci. Eng. 35 (1993) 457–481.
[3] M. Schelef, G.W. Graham, Catal. Rev. Sci. Eng. 36 (1994) 433–457.
[4] J. Gustafon, R. Westerström, A. Resta, A. Mikkelsen, J.N. Andersen, O. Balmes, X. Torrelles, M. Schmid, P. Varga, B. Hammer, G. Kresse, C.J. Baddeley, E. Lundgren, Catal. Today 145 (2009) 227–235.
[5] H. Wang, M. Yan, Z. Jiang, Thin Solid Films 401 (2001) 211–215.
[6] K.T. Jacob, M.V. Sriram, Metall. Mater. Trans. A 25A (1994) 1347–1357.
[7] K.T. Jacob, T. Uda, T.H. Okabe, Y. Waseda, High Temp. Mater. Process. 19 (2000) 11–16.
[8] L. Wöhler, N. Jochum, Z. Physik. Chem. A 167 (1933) 169–179.
[9] O. Muller, R. Roy, J. Less Common Met. 16 (1968) 129–146.
[10] J.H. Norman, H.G. Staley, W.E. Bell, J. Phys. Chem. 68 (1964) 662–663.
[11] C.B. Alcock, G.W. Hooper, Proc. R. Soc. Lond. A 254 (1960) 551–561.
[12] J.E. Hurst Jr., B.K. Harrison, Chem. Eng. Commun. 112 (1992) 21–30.
[13] J. Leitner, P. Chuchvalec, D. Sedmidubsky, Chem. Listy 95 (2001) 2–8.
[14] G. Periaswami, S.V. Varamban, S.R. Babu, C.K. Mathews, Solid State Ionics 26 (1988) 311–317.
[15] L.B. Pankratz, Thermodynamic Properties of Elements and Oxides, Bulletin 677, United States Department of the Interior, Bureau of Mines, 1984.
[16] O. Kubaschewski, C.B. Alcock, Metallurgical Thermochemistry, 5th ed., Pergamon Press, New York, 1979, 185 pp.
[17] O. Knacke, O. Kubaschewski, K. Hesselmann, Thermodynamic Properties of Inorganic Substances, Springer-Verlag, Berlin, 1991.
[18] K.T. Jacob, S. Mishra, Y. Waseda, J. Am. Ceram. Soc. 83 (2000) 1745–1752.
[19] M.E. Grillo, Comput. Mater. Sci. 33 (2005) 83–91.